

1 GIS-models with fuzzy logic for Susceptibility Maps of debris flow using multiple types of parameters: A Case Study
2 in Pinggu District of Beijing, China

3 Yiwei Zhang¹, Jianping Chen^{1,*}, Qing Wang¹, Chun Tan^{2,3}, Yongchao Li^{4,5,6}, Xiaohui Sun⁷, Yang Li⁸

4
5 1 College of Construction Engineering, Jilin University, Changchun 130026, China

6 2 China Water Northeastern Investigation, Design and Research Co., Ltd, Changchun, Jilin 130026, China

7 3 North China Power Engineering Co., Ltd. of China Power Engineering Consulting Group, Changchun, Jilin 130000,
8 China

9 4 Key Laboratory of Shale Gas and Geoengineering, Institute of Geology and Geophysics, Chinese Academy of
10 Sciences, China.

11 5 University of Chinese Academy of Sciences.

12 6 Innovation Academy for Earth Science, Chinese Academy of Sciences, China.

13 7 Department of Earth Sciences and Engineering, Taiyuan University of Technology, Taiyuan 030024, China

14 8 Beijing institute of geological and prospecting engineering, Beijing 100020, China

15 * Corresponding author. Tel.:+86 13843047952

16 * Email address: chenjp@jlu.edu.cn

17
18
19 **Abstract**

20 Debris flow is one of the main causes of life loss and infrastructure damage in mountainous areas. This hazard
21 should be recognized in the early stage of land development planning. According to field investigation and expert
22 experience, a scientific and effective quantitative susceptibility assessment model was established in Pinggu District
23 of Beijing. This model is based on Geographic Information System (GIS), combining with grey relational, data-
24 driven and fuzzy logic methods. The influence factors, which are divided into two categories and consistent with the
25 system characteristics of debris flow gully, are selected, also a new important factor is proposed. The results of the
26 17 models are verified using data published by the authority, and validated by two other indexes as well as Area
27 Under Curve (AUC). Through the comparison and analysis of the results, we believe that the streamlining of factors
28 and scientific classification should attract attention from other researchers to optimize a model. We also propose a
29 good perspective to make better use of the watershed feature parameters. These parameters fit well with the watershed
30 units. With full use of insufficient data, scientific calculation, and reliable results, the final optimal susceptibility map
31 could potentially help decision makers in determining regional-scale land use planning and debris flow hazard
32 mitigation. The model has advantages in economically backward areas with insufficient data in mountainous areas
33 because of its simplicity, interpretability and engineering usefulness.

34 Key words: debris flow; susceptibility assessment; fuzzy logic; model optimization; hazard mitigation

36 **1 Introduction**

37 Debris flows are processes of rapid transport of water and soil materials in mountain watersheds, with sudden
38 and destructive outbreaks(Di et al., 2019). Some debris flows can often cause devastating disasters and huge
39 losses(Zhang et al., 2021) and seriously threaten the lives and properties of people in the mountains, the safety of
40 major projects, and restrict social and economic development (Iverson, 1997; Hungr et al., 2005; Hu et al., 2011;
41 Takahashi, 2014; Wu et al., 2019). Mass movements in Beijing range in scale from shallow slope failures and rockfalls
42 to catastrophic rock avalanches frequently mobilize to form debris flows, threatening the ecological environment of
43 the mountainous area (Zhong et al., 2004). Especially, in recent years, due to the superposition of extreme rainstorm
44 weather and human engineering activities, debris flow events have increased gradually(Li et al., 2021b). As the capital
45 of China, Beijing also has strong influence and radiation at home and abroad, where geological disasters are widely
46 concerned (Xie et al., 2004; Li et al., 2020b). With the deepening understanding of debris flow disaster and the
47 updating of database, a new and more accurate evaluation is also very necessary. Therefore, it is of great significance
48 to establish accurate and scientific debris flow susceptibility map.

49 Through previous studies, it can be summarized that the current research on debris flow mainly focuses on the
50 following aspects: study on mechanism of debris flow, study on early warning and prediction of debris flow, study
51 on numerical simulation of debris flow and study on debris flow hazard analysis. Especially, studies on debris flow
52 hazard analysis have raised the attention of the researchers as soon as it appears(Dong et al., 2009). Communicating
53 information about debris flow hazard analysis is a crucial component of preparedness and hazard mitigation (Chiou
54 et al., 2015). Susceptibility assessment, an important part of a hazard assessment of geological processes, is more
55 flexible(Li et al., 2021a). In the early days, the susceptibility assessment of debris flows was mainly qualitative
56 research using geomorphological information (Guzzetti et al., 1999). In 1976, the United Nations commissioned the
57 International Union of Engineering Geology to conduct a risk assessment of debris flows, which marked the
58 beginning of research on the susceptibility assessment of debris flows as an important research direction for disaster
59 prevention and prediction (Li et al., 2020b). Many methods and techniques have been proposed to evaluate debris
60 flow susceptibility assessment based on different qualitative and quantitative approaches along with geo-
61 environmental information (Liu and Wang, 1995), Such as the analytic hierarchy process (Wu et al., 2016), logistic
62 regression method (Regmi et al., 2013; Conoscenti et al., 2015), information value (Akbar and Ha, 2011; Melo et al.,
63 2012), support vector machine(Pourghasemi et al., 2017), frequency ratio (FR) (Sun et al., 2018), certainty factor
64 (CF) (Tsangaratos and Ilia, 2015), neural network (Lee et al., 2003; Liu et al., 2005) and Bayesian network algorithm
65 (Liang et al., 2012; Tien Bui et al., 2012), etc. These methods have corresponding advantages and limitations for
66 research subjects with different geological conditions. Generally speaking, it is easier to get satisfactory results by
67 combining and comparing various methods (Meyer et al., 2014; Di Napoli et al., 2020; Fang et al., 2020). In summary,
68 with the development of mathematical theory, the susceptibility assessment of debris flows has been extensively and
69 quantitatively studied, and the research methods have also changed from single to comprehensive.

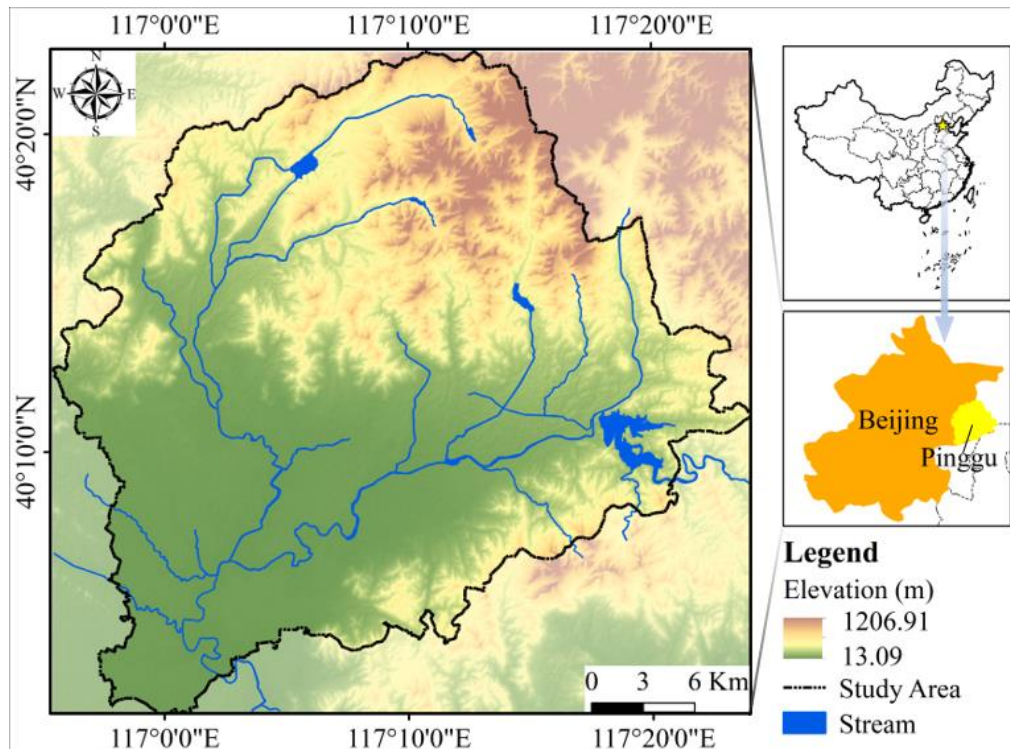
70 The economy in mountainous areas is often backward, we cannot supervise and verify every basin due to limited
71 funds. The debris flow susceptibility assessment can give decision makers a basis for rational allocation of resources,
72 and determine which gullies should be focused on. In other words, the study plays a link role for other studies.

73 Recently, with the development of mathematical theory, computer technology, the application of 3S (Remote sensing,
74 Geography information systems, Global positioning systems), the susceptibility assessment of debris flows has been
75 extensively and quantitatively studied(Li et al., 2020a). As research progresses, debris flows are increasingly seen as
76 an open system. There are many factors influencing the system and the combination of factors is non-linear and the
77 interactions are chaotic. Therefore, it is very difficult to find a unified and standard evaluation model. At present,
78 when the information is insufficient, field investigation and experience of experts are necessary. However, the
79 experience is often subjective and needs a lot of professional experience accumulation. It is very important to express
80 the experience of experts objectively and understandably to serve decision makers. The application of fuzzy set theory
81 in GIS environments is effective for similar problems(Luo and Dimitrakopoulos, 2003; Porwal et al., 2006).

82 The main objective of this paper is to propose a quantitative geographic information system (GIS)-based model.
83 The results of expert experience scoring and site surveys are used as guidance and reference in the modelling process.
84 We have tried to apply methods that can indicate the non-linearity of the debris flow system. Finally, the modelling
85 process should respect the laws of geomorphological evolution and the geological basis. Otherwise, the result will
86 tend to be simply data fitting(Porwal et al., 2006).

87 **2 Study area**

88 The study area is located on the northeast of Beijing, China (Fig. 1), with a total area of 948.24 square kilometers.
89 The elevation of Pinggu is high in the northeast and low in the southwest. It is surrounded by mountains, accounts
90 for about two-thirds of the total area, on three sides in the southeast and north. The central and southern parts are
91 alluvial plains. The area, geologically, is the west extension of the famous Jixian section, whose bedrock is mainly
92 Middle and Late Proterozoic dolomite(Lü et al., 2017). The administrative unit of Pinggu District is used as the study
93 area boundary, mainly considering that geological hazards frequently influence human economic activities, so
94 political factors must be taken into account. And within the administrative region, inconsistent decision-making can
95 be effectively avoided.

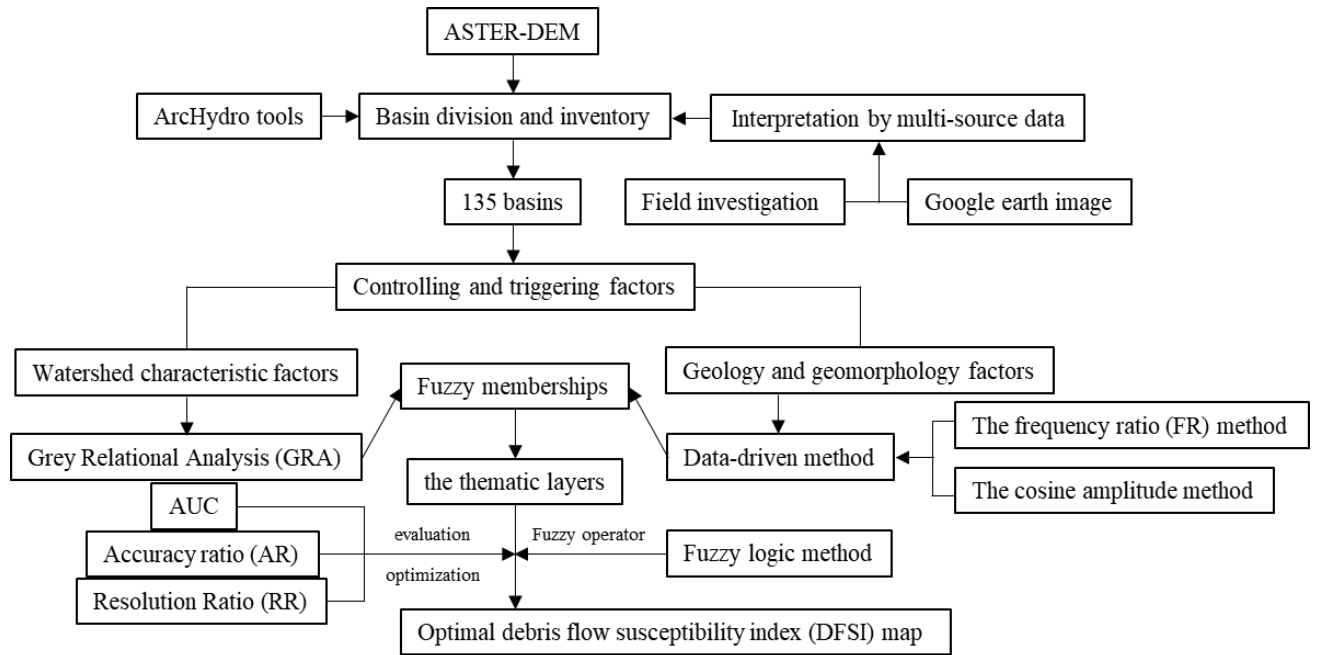


96 Fig. 1 Study area
97

98 **3. Data and Methodology**

99 In this study, the susceptibility assessment of debris flow hazard was based on the drainage basin unit. In such
100 a model, hydro-logical response unit can fully represent the hydrological process of hillside and will make the results
101 more meaningful(Khan et al., 2013; Khan et al., 2016; Zou et al., 2019). First, drainage networks were extracted from
102 the ASTER-DEM by using the ArcGIS ArcHydro Toolbox and regions without obvious watershed characteristics
103 were directly deleted. Then for each drainage basin, 19 controlling and triggering factors divided into two types were
104 calculated. In addition, for these factors have different characteristics, different methods were used to calculate the
105 fuzzy membership for different type factors. Field investigation is generally required in geological hazard surveys. If
106 these data are applied to the model, it can help with the model building and reduce the time for model training. The
107 weights derived from the grey relational analysis method used in the following section (section 3.4.1) are based on
108 the data from the field investigation. While geology and geomorphology factors are independent of watershed
109 characteristics, it is suitable to use statistical methods to determine the objective weight. Finally, the debris flow
110 susceptibility index (DFSI) map was derived by overlaying the factor thematic layers with fuzzy logic method. The
111 workflow of debris flow susceptibility assessment is showed in Fig.2. First, a DEM map of the Pinggu area was
112 downloaded. Then, the basin units were generated from the DEM map using the ArcHydro tool. The derived results
113 were analyzed and units that did not fit the characteristics of the watershed were removed. During the analysis, the
114 field investigation data and Google images were referenced. After that, the controlling and triggering factors for the
115 remaining 135 catchments were counted. For the fuzzy memberships, watershed characteristic parameters were
116 determined by grey correlation, the geological and geomorphological factors were determined by the frequency ratio
117 (FR) method and the cosine amplitude method. Finally, the individual layers were overlaid by fuzzy logic operations
118 to obtain the final map. As there were different combinations of factors, 17 results were derived. Three indexes (AUC,

119 AR and RR) were used to evaluate advantages and disadvantages of these results.



120
121 Fig.2 Workflow of debris flow susceptibility assessment

122 **3.1 Debris flow basin division and inventory**

123 There are many geological hazard points in mountainous area, so it is not realistic to monitor them completely
 124 by professional teams. According to the monitoring and preventing staff and the villagers, the detailed field
 125 investigation (Fig.3) for the evidence collection of debris flows will be carried out at the reported disaster point,
 126 aiming at record the loose material, delineating the basin and exploring other important information of the debris
 127 flow gullies. Moreover, field investigation is also very important for model modification. Then based on the
 128 Hydrology module in ArcGIS 10.2, the research object can be determined. Compared with grid unit and slope unit,
 129 hydrological response unit for susceptibility of debris flow has greater advantages(Li et al., 2021b; Zou et al., 2019).
 130 Finally, referring to the result of the field investigation and the remote sensing image, 135 basins are divided after
 131 removing the flat and irregular areas (Fig. 4), and 48 basins of them were investigated on field, accounting for 36%.

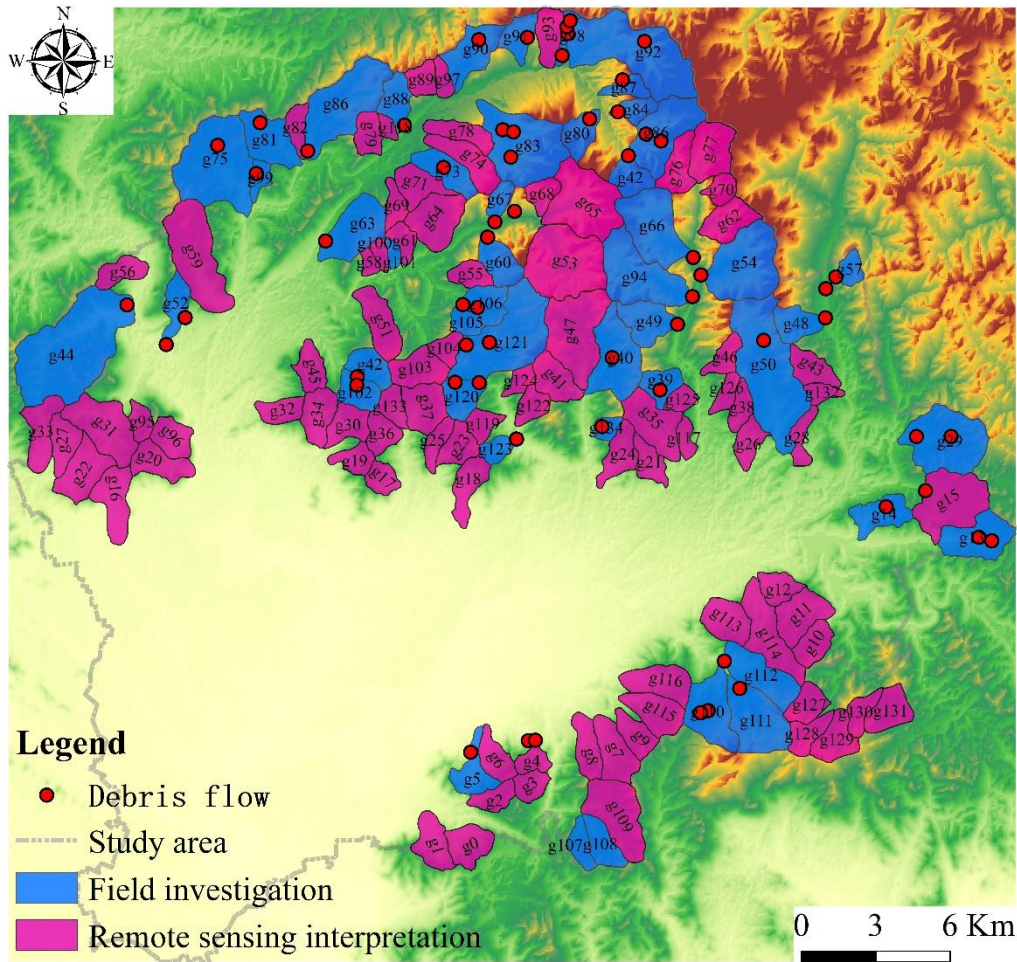


132

133 Fig.3 Field investigation photos. **a** Loose material; **b** Middle and Late Proterozoic dolomite; **c** colluvium deposit; **d**

134 Slope fracture; **e** Channel erosion phenomenon

135



136

137 Fig. 4 Debris flow basin division and inventory.

138 Note: The data of debris flow points comes from Beijing Municipal Commission of Planning and Natural Resources
 139 websites (http://ghzrzyw.beijing.gov.cn/zhengwuxinxi/zxzt/dzzhfztt/zzzhdcpg/202008/t20200807_1976436.html)

140 **3.2 Debris flow controlling and triggering factors**

141 The basic requirement for the assessment of debris flows is that some factors included are easily obtainable,
 142 meaningful for susceptibility assessment, and can be used for evaluating the need for passive or active debris flow
 143 mitigation. According to previous studies, 19 factors are selected in this study. the factors are divided into two types
 144 (Table 1) because of their different characteristics. Watershed characteristic factors (Type A) can be directly
 145 quantified, once the basin is determined (Fig. 5). The influence of these parameters is bounded by the watershed;
 146 Geology and geomorphology factors (Type B) need to be further processed, even if the watershed is determined. The
 147 scope of these parameters is independent of the watershed boundary.

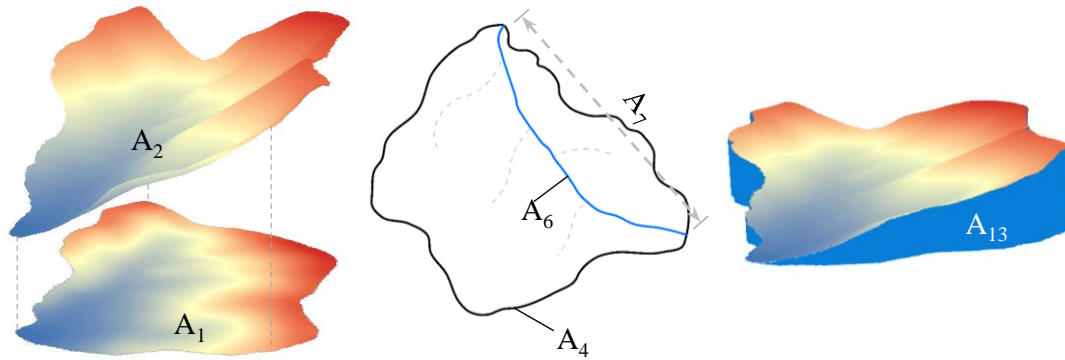
148

Table 1 Factors for susceptibility assessment

Factors and Description		Significance	obtaining ways
A ₁	The planimetric (projected) area of the catchment	Geometric parameter; affecting the accumulative total volume of water and representing the potential magnitude(Zhang et al., 2011; Cao et al., 2016; Chang and Chien, 2007)	derived from DEM
A ₂	The curved surface area of the catchment	Real contact area between rainfall and basin	derived from DEM
A ₃	The surface roughness of the catchment	Dimensionless parameters, reflecting the fragmentation degrees of the surface and the ground surface micro-topography. Wu et al. (2019) believe the factor can further reflects the ability of the earth to resist wind erosion.	Calculated by $A_3 = A_2 / A_1$
A ₄	The perimeter of catchment	Geometric parameter, controlling the boundaries of a watershed	derived from DEM
A ₅	Form factor	Hydrologic parameter, related to the distribution of flow rate hydrograph(Chang and Chien, 2007)	Calculated by $A_5 = \frac{A_4}{2\sqrt{\pi A_1}}$
A ₆	The curve length of the main channel	Importance for the travel distance of materials and affecting the potential of erosive agents to dislodge and transport materials(Gómez and Kavzoglu, 2005)	derived from DEM
A ₇	The straight length of the main channel	Geometric parameter, representing the change of material source in space	derived from DEM
A ₈	Bending coefficient of the main channel	Affecting the discharge situation of debris flows(Li et al., 2020a; Zhang et al., 2013)	Calculated by $A_8 = A_6 / A_7$
A ₉	The gradient of the main channel	Hydraulic gradient parameter, affecting water transport capacity	Calculated by $A_9 = A_{12} / A_6$
A ₁₀	Maximum elevation in the catchment	Affecting vegetation and bedrock exposure	derived from DEM
A ₁₁	Minimum elevation in the catchment	Affecting vegetation and bedrock exposure slightly	derived from DEM
A ₁₂	Maximum relative relief in the catchment	The higher the value of A ₁₂ is, the large relative relief provides favorable terrain conditions for the initiation of the debris flow source.	Calculated by $A_{12} = A_{10} - A_{11}$
A ₁₃	Basin volume: the volume above the level of the minimum elevation in the basin	Representing the maximum material source that can be produced in an ideal state, loose material volume	derived from DEM
A ₁₄	Drainage density	Representing the geological structure, lithology, and the degree of rock weathering comprehensively and affecting the	the ratio of the total length of river network lines to A ₁

range of lateral erosions and retrogressive(Cao et al., 2016; Zhang et al., 2011)				
Geology and geomorphology factors (Type B)	B ₁	Lithology	Affecting the rock mass shear strength and permeability (Donati and Turrini, 2002)	derived from 1:50,000 geological maps
	B ₂	Proximity to faults	correlated with slope failures by generally reducing the strength of the rock mass (Dramis and Sorriso-Valvo, 1994; Korup, 2004; Kellogg, 2001; Kritikos and Davies, 2015).	derived from 1:50,000 numerical geological maps
	B ₃	Slope (degrees)	correlated with the probability of landslide occurrence (Dai and Lee, 2002; Lee and Choi, 2004; He and Beighley, 2008). The greater the slope, the greater the vertical component of gravity (Donati and Turrini, 2002), and the higher frequency of slope failures (Lee and Sambath, 2006; Lee and Talib, 2005)	derived from DEM
	B ₄	Slope aspect	affecting slope instability directly or indirectly, as a result of drying winds, sunlight, rainfall and vegetation (Dai and Lee, 2002; Dai et al., 2001).	derived from DEM
	B ₅	Curvature	Affecting slope stability. While Lee and Talib (2005) and Ohlmacher (2007) argue on how curvature affect slope stability.	derived from DEM

150 Note: The geological maps are provided by Beijing institute of geological and prospecting engineering and the digital elevation model-(DEM) of study area are from
151 SRTM-DEM with a resolution of 30 m ([http://gdex. cr. usgs. gov/gdex/](http://gdex.cr.usgs.gov/gdex/)).
152



153
 154 Fig. 5 Graphical illustration of some Type A factors. A_1 is the planimetric (projected) area of the catchment; A_2 is
 155 the curved surface area of the catchment; A_4 is the perimeter of catchment; A_6 is the curve length of the main channel;
 156 A_7 is the straight length of the main channel; A_{13} is basin volume

157 3.3 Fuzzy logic in susceptibility modelling

158 Fuzzy set theory is proposed by Zadeh (1965). It is an efficient way of expressing the concept of partial set
 159 membership degree. This concept differs from classical binary (0-1 value) logic. More words with a transitional fuzzy
 160 descriptions (such as low, medium, and high) are used (Kritikos and Davies, 2015). This fuzzy expression is
 161 particularly applicable to geological hazard classification. In the theory of fuzzy sets, elements have different degrees
 162 of membership in the interval [0,1]. 1 represents complete membership, and 0 represents non membership. Ross
 163 (1995) showed that fuzzy systems are useful in two general situations (Kritikos and Davies, 2015). The method is
 164 very consistent with the characteristics of debris flow system, whose predisposing factors are fuzzy in nature and
 165 mechanism is complex and not fully understood. Application of fuzzy logic method, the critical step is to find the
 166 suitable fuzzy membership of factors. And fuzzy membership degree is equivalent to the weight in expert scoring
 167 method, which is calculated by objective method rather than given subjectively.

168 3.4 Fuzzy memberships

169 3.4.1 Grey Relational Analysis (GRA) in susceptibility modeling

170 GRA is proposed by Deng (1982) and it is an important part of grey system theory (Wang et al., 2014).
 171 Comparing with mathematical statistics methods which need lots of sample data, typical probability distribution and
 172 large calculation, GRA is applicable to small sample size with the data whether regular or not. There will be no
 173 inconsistency between qualitative analysis and quantitative analysis (Deng, 1988). Besides it is to excoitate the
 174 leading and potential factors that affect the development of the system, and quantitatively describe the development
 175 and change trend of the system by studying whether the relative change trend of the grey factor variables with
 176 complex relationship is consistent in the process of system development and evolution (Liu et al., 2004). Thus, grey
 177 correlation analysis is introduced to quantify the correlation between each factor and the evaluation results according
 178 to field investigation expert experience. First, the procedure of GRA is to translate the performance of every
 179 alternative into a comparability sequence (Lin and Lin, 2002; Kuo et al., 2008; Wei et al., 2017). Therefore, according
 180 to technical standard, "Specification of geological investigation for debris flow stabilization (DZ/T0220-2006)",
 181 published by the China Ministry of Lands and Resources, the preliminary assessment results of debris flow

182 susceptibility are obtained, which are used as the reference sequence of grey relation method (Table 2). Second, the
 183 grey correlation coefficient of all A factors is calculated by Eq. (1). Finally, the average grey relational coefficient
 184 (the correlation degree) is calculated by Eq. (2) as the fuzzy memberships (Table 3).

$$185 \quad \xi_i(k) = \frac{\min_k \min |x_0(k) - x_i(k)| + 0.5 \max_k \max |x_0(k) - x_i(k)|}{|x_0(k) - x_i(k)| + 0.5 \min_k \min |x_0(k) - x_i(k)|} \quad (1)$$

186 Where $\xi_i(k)$ is the grey relational coefficient, $i=1, 2, \dots, n$ are the number i type A factors, $k=1, 2, \dots, n$ are the
 187 number of basins, $x_0(k)$ is the reference sequence (ideal target sequence), $x_i(k)$ is the number i type A factor sequence

$$188 \quad r_i = \frac{1}{N} \sum_{k=1}^n \xi_i(k) \quad (2)$$

189 Where r_i is the correlation degree in the range (0,1). N is the total number of basins in Table 2

Table 2 Quantitative evaluation grade standard table for Debris flow susceptibility

name	g5	g13	g14	g29	g39	g40	g42	g44	g48	g49	g50	g52	g54
score	59	54	50	63	61	66	55	65	78	69	85	46	70
name	g57	g60	g63	g66	g67	g72	g73	g75	g80	g81	g83	g84	g85
score	56	63	58	73	62	84	62	67	84	69	80	75	86
name	g86	g87	g88	g90	g91	g92	g94	g98	g99	g101	g102	g105	g106
score	73	84	60	70	80	84	71	78	61	65	67	65	70
name	g107	g108	g110	g111	g112	g120	g121	g123	g134	-	-	-	-
score	45	45	69	69	74	62	63	73	56	-	-	-	-

190 Note: ($130 \geq \text{score} \geq 116$, VH) , ($115 \geq \text{score} \geq 87$, M) , ($86 \geq \text{score} \geq 44$, L) , ($43 \geq \text{score} \geq 15$, N)

191 VH=very high susceptibility, M=moderate susceptibility, L=low susceptibility, N= Non-debris flow

192

193 Table 3 The fuzzy memberships of type A factors

Factor	A ₁	A ₂	A ₃	A ₄	A ₅	A ₆	A ₇
Fuzzy membership	0.77	0.77	0.63	0.6	0.54	0.55	0.67
Factor	A ₈	A ₉	A ₁₀	A ₁₁	A ₁₂	A ₁₃	A ₁₄
Fuzzy membership	0.71	0.55	0.55	0.59	0.61	0.79	0.54

194

195 3.4.2 Data-driven method in susceptibility modeling

196 landslide is one of the main fixed sources of debris flow in mountainous area. Shallow landslides are one of the
 197 most common categories of landslides. They frequently involve large areas and different soils in various climatic
 198 zones (Benda and Dunne, 1987; Selby, 1982; Borrelli et al., 2014). Great debris flows may result from numerous,
 199 small slope failures that subsequently coalesce (Fairchild, 1987; Roeloffs, 1996), from flow enlargement due to
 200 incorporation of bed and bank debris (Pierson et al., 1990; Bovis and Dagg, 1992), or from large, individual landslides
 201 that mobilize partially or almost totally (Vallance and Scott, 1997; Iverson et al., 1997). Debris flows may also scour
 202 steep channels to bedrock and accelerate sediment delivery to downstream, lower-gradient channels. The spatial and
 203 temporal distribution of shallow landslides are important controls on landscape evolution and a major component of
 204 both natural and management-related disturbance regimes in mountain drainage basins (Tsukamoto et al., 1982;
 205 Dietrich et al., 1986; Benda, 1987; Crozier et al., 1990). Therefore, the landslide susceptibility assessment methods
 206 can be used for reference to debris flow susceptibility assessment.

207 For type B factors which cannot be characterized by a specific number, the frequency ratio (FR) method and the

208 cosine amplitude method can be used to derive their fuzzy memberships. The FR ratio defined as Eq. (3). Considering
 209 the fuzzy membership must be in the interval [0,1], the FR values of the different categories are normalized by the
 210 largest FR value (Lee, 2006; Pradhan, 2010, 2011a, b) within the same type factor (Table 4) in order to derive the
 211 function.

$$212 \quad FR = \frac{N_{(Di)}/N_{(Ci)}}{N_{(D)}/N_{(A)}} \quad (3)$$

213 where $N_{(Di)}$ is the number of debris flow pixels in the category i , $N_{(Ci)}$ is the total number of pixels in the category
 214 i , $N_{(D)}$ is total number of debris flow pixels in the study area, and $N_{(A)}$ is the total number of pixels in the study area.
 215

216 The cosine amplitude method (Ross, 1995) is also widely used (Ercanoglu and Gokceoglu, 2004; Kanungo et
 217 al., 2006; Kanungo et al., 2009; Ercanoglu and Temiz, 2011) to establish relationships among elements of two or
 218 more datasets (Kritikos and Davies, 2015). Assuming that n is the number of data samples (categories of a factor
 219 used in the analysis) represented as an array $X = \{x_1, x_2, \dots, x_n\}$ and that each of its elements, x_i , is a vector of length
 220 m (i.e. the size of the raster image) and can be expressed as $X = \{x_{i1}, x_{i2}, \dots, x_{im}\}$, then each element of a relation r_{ij}
 221 results from a pairwise comparison of a factor category x_i with a category of the debris flow distribution layer x_j
 222 (debris flow or non-debris flow). The memberships can be calculated by Eq. (4):

$$223 \quad r_{ij} = \frac{|\sum_{k=1}^m x_{ik}x_{jk}|}{\sqrt{(\sum_{k=1}^m x_{ik}^2)(\sum_{k=1}^m x_{jk}^2)}} \quad (4)$$

224 Analogy with the study of Kanungo et al. (2006), we defined the r_{ij} value for any given factor category as the
 225 ratio of the total number of debris flow pixels in the category to the square root of the product of the total number of
 226 pixels in that category and the total number of debris flow pixels in the area. Values of r_{ij} close to 1 indicate similarity
 227 whereas values close to 0 indicate dissimilarity between the two datasets (Kritikos and Davies, 2015). What's more,
 228 every thematic layer must use the same pixel size to use the method properly.
 229

Table 4 Factor categories and their fuzzy membership degrees

Factor	Factor class	Number of pixels	Number of pixels %	Number of pixels classified as debris flows	Number of pixels classified as debris flow %	Frequency ratio (FR)	Normalized frequency ratio	r_{ij}	Comprehensive ratio (FRR)
Lithology	Quaternary sediments-unconsolidated clastic sediments	7562017	0.320	48190	0.017	0.026	0.021	0.091	0.002
	Coarse-grained sediments	1148321	0.049	21741	0.008	0.076	0.063	0.061	0.004
	Medium-grained sediments	259619	0.011	12013	0.004	0.186	0.154	0.045	0.007
	Fine-grained sediments	754655	0.032	76380	0.027	0.407	0.337	0.114	0.038
	High-grade metamorphics	986435	0.042	154332	0.055	0.629	0.522	0.162	0.085
	Granitoids	725651	0.031	140936	0.050	0.781	0.648	0.155	0.100
	Mafic extrusive	75495	0.003	16398	0.006	0.873	0.724	0.053	0.038
	Terrigenous clastic rock	3289458	0.139	986495	0.352	1.205	1.000	0.41	0.410
proximity to faults	Limestones	8804379	0.373	1343754	0.480	0.614	0.509	0.478	0.243
	<100	1057209	0.045	231016	0.083	0.878	1.000	0.198	0.198
	100-500	3778095	0.160	774566	0.277	0.824	0.938	0.363	0.341
	500-1000	3894600	0.165	716963	0.256	0.740	0.842	0.349	0.294
	1000-2000	5707265	0.241	760699	0.272	0.536	0.610	0.36	0.220
	2000-3000	2749240	0.116	246925	0.088	0.361	0.411	0.205	0.084
slope (degrees)	>3000	6421103	0.272	69382	0.025	0.043	0.049	0.109	0.005
	0-5	9674508	0.410	153889	0.055	0.064	0.056	0.162	0.009
	5-10	2815606	0.119	383198	0.137	0.547	0.480	0.255	0.123
	10-15	2955913	0.125	521040	0.186	0.709	0.622	0.298	0.185
	15-20	2879704	0.122	570515	0.204	0.797	0.699	0.312	0.218
	20-25	2432724	0.103	498303	0.178	0.824	0.723	0.291	0.210
	25-30	1620325	0.069	350686	0.125	0.870	0.764	0.244	0.187
	30-35	837185	0.035	209574	0.075	1.007	0.883	0.189	0.167
	35-40	294141	0.012	82000	0.029	1.121	0.983	0.118	0.116
	40-45	77038	0.003	21133	0.008	1.103	0.968	0.06	0.058
Slope aspect	>45	30091	0.001	8529	0.003	1.140	1.000	0.038	0.038
	Flat	380875	0.016	463	0.000	0.005	0.005	0.009	0.000
	North	2370048	0.100	296900	0.106	1.006	1.000	0.318	0.111
	Northeast	2193998	0.093	279917	0.100	0.513	0.510	0.218	0.092
	East	2873308	0.122	295555	0.106	0.414	0.411	0.224	0.111

	Southeast	3122267	0.132	353489	0.126	0.455	0.453	0.245	0.108
	South	3219111	0.136	354420	0.127	0.443	0.440	0.246	0.133
	Southwest	3144353	0.133	400064	0.143	0.512	0.509	0.261	0.135
	West	3525895	0.149	436381	0.156	0.498	0.495	0.273	0.140
	Northwest	2787380	0.118	381679	0.136	0.551	0.547	0.255	0.318
Curvature	Concave	490900	0.021	109157	0.039	0.893	1.000	0.136	0.136
	Less concave	2037602	0.269	394583	0.141	0.778	0.871	0.259	0.226
	Flat	18364429	15.992	1769210	0.631	0.387	0.433	0.549	0.238
	Less convex	2202019	8.482	416142	0.149	0.759	0.850	0.266	0.226
	Convex	522285	0.692	112740	0.040	0.867	0.971	0.139	0.135

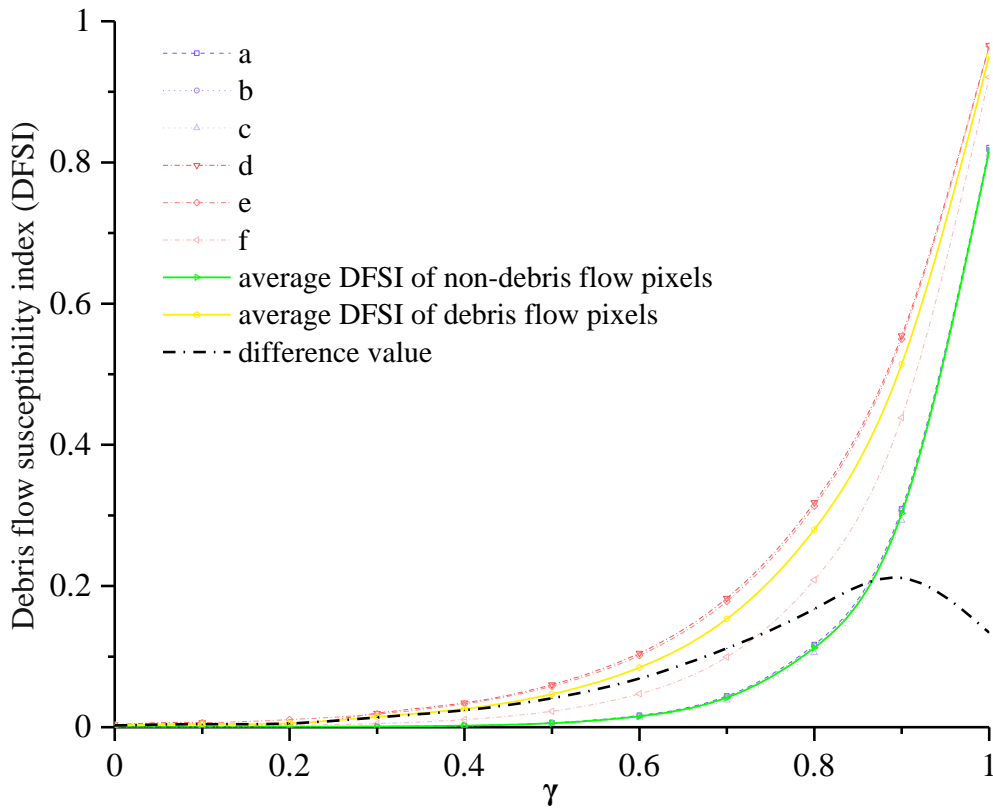
231

232 **3.5 DFSI map**

233 To derive the debris flow susceptibility index (DFSI) map by overlaying the factor thematic layers using fuzzy
 234 logic method, the "fuzzified" factors represented by information layers in raster format with values ranging from 0
 235 to 1 need to be combined. Compared with other four fuzzy operators, Fuzzy Gamma (Eq.5) is more suitable for the
 236 research (Kritikos and Davies, 2015). To determine the appropriate γ value, the results of different gamma values
 237 were compared by the greatest distance (Kritikos and Davies, 2015) between the average DFSI curves of the debris
 238 flows locations and non-debris flows locations (For example, flat pixels)(Fig. 6). Finally, 0.9 is determined for the γ
 239 value, because there is the greatest difference between debris flow and non-debris flows locations areas. In order to
 240 illustrate the superiority of our model through comparison, 17 results are calculated in ArcGIS.

241
$$\mu_{(x)} = (1 - \prod_{i=1}^n (1 - \mu_i))^\gamma * (\prod_{i=1}^n \mu_i)^{1-\gamma} \quad (5)$$

242 where $\mu_{(x)}$ is the combined membership value, μ_i is the fuzzy membership function for the i th map, $i=1,2, \dots, n$
 243 are the numbers of thematic layers to be combined, and γ is a parameter in the range (0,1).



244 Fig. 6 Effect of γ value on Debris flow susceptibility index (DFSI). Curves d, e and f correspond to debris flow pixels,
 245 and curves a, b and c correspond to non-debris flow area where a Debris flow is unlikely. According to curve i, the
 246 maximum difference between the average DFSI values is observed for $\gamma \approx 0.9$
 247

248 To find the optimal model, 17 results were compared (Table 5). According to the distribution map of potential
 249 geological hazard points and susceptibility map in Pinggu District published by Beijing Municipal Commission of
 250 Planning and Natural Resources(Bmcp&Nr, 2020), three indexes are used to verify the validity and accuracy of the
 251 model.
 252

253 The results of the model are independent of the model itself, so the predictive performance of the final map is

254 not just “the goodness of fit” of the data (Chung et al., 1995; Remondo et al., 2003). A relatively reliable technique
 255 for quantitatively assessing how well a model is the construction of validation or success rate curves (Chung and
 256 Fabbri, 1999; Westen et al., 2003; Remondo et al., 2003; Frattini et al., 2010) based on a comparison between the
 257 spatial distribution of debris flows and modelled debris flow susceptibility. The curves illustrate the debris flow
 258 recorded in the area with respect to susceptibility values also expressed as cumulative percentages of the total area.
 259 The area under the curve (AUC) defines the success rate (Marjanović et al., 2011). Generally, AUC values above 0.7
 260 indicate model performance can be acceptable, while below 0.7, the performance is considered poor (Kritikos and
 261 Davies, 2015).

262 Although AUC is an effective evaluation method, the results are not comprehensive as mathematical features
 263 for selecting the best measurement model because of insufficiency data for validation. In order to ensure the
 264 objectivity of the results, we can only effectively use the recorded debris flow gully as positive, while the others as
 265 negative. Thus, a two-category test is proposed to verify the model in this paper. First, the DFSI map of each model
 266 are divided into two categories by Natural Breaks (Jenks) method (Fig. 7). Then the accuracy ratio (AR) is defined
 267 as the frequency of the number of debris flow both classified by model and simultaneously recorded in site to the
 268 number of debris flow recorded in site. The Resolution Ratio (RR) is defined as the number of debris flow
 269 classified by model and simultaneously recorded in site to the total number debris flow classified by the model (in
 270 red color). Take R₄ for example, there are total 135 basins in the research area, but only 46 records of debris flows
 271 (Fig.3). And in the results of two categories by Natural Breaks (Jenks) method, 20 basins are divided in to debris
 272 flow, while there are only 14 debris flows among them. Then AR is calculated by dividing 14 into 46 and RR was
 273 calculated by dividing 14 into 20.

274 The higher the two values, the better the susceptibility map. Finally, the performance of models (P value) can
 275 be obtained by the Eq. (6). AUC values less than 0.6 are directly eliminated. Comparing the results of rest models,
 276 the result of R₁₆ is optimal, and the results of DFSI map are in good agreement with those of field investigation
 277 (Fig. 8).

$$278 \quad P = AUC + \sqrt{(AR * RR)} \quad (6)$$

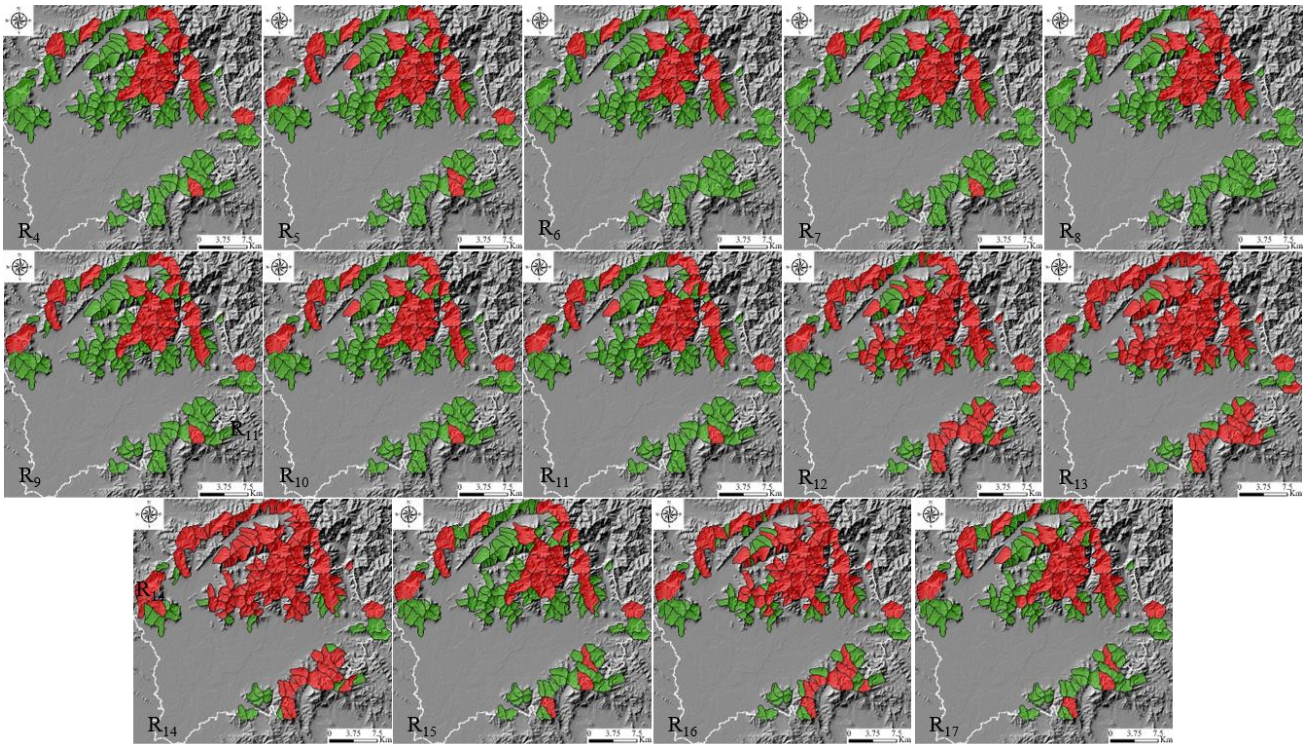
279 Table 5 Predictive performance of different models

Result and Description			AUC	Two-category test		Performance index (centesimal grade)
				Accuracy Ratio (AR)	Resolution Ratio (RR)	
A factors only or B factors only	R ₁	B factors with r _{ij}	0.460	/	/	/
	R ₂	B factors with FR	0.687	/	/	/
	R ₃	B factors with FRR	0.602	/	/	/
	R ₄	All A factors	0.786	0.304	0.700	83
	R ₅	Selected A factors	0.760	0.391	0.750	94
All factors as a single thematic layer	R ₆	All A factors and B factors with r _{ij}	0.776	0.261	0.667	74
	R ₇	All A factors and B factors with FR	0.779	0.283	0.684	78
	R ₈	All A factors and B factors with FRR	0.753	0.326	0.600	76
	R ₉	Selected A factors and B	0.746	0.348	0.727	86

		factors with r_{ij}				
	R ₁₀	Selected A factors B factors with FR	0.761	0.348	0.727	87
	R ₁₁	Selected A factors B factors with FRR	0.740	0.348	0.727	85
A factors combined into one thematic layers, B factor combined into another thematic layers	R ₁₂	All A factors and B factors with r_{ij}	0.708	0.5	0.511	82
	R ₁₃	All A factors and B factors with FR	0.753	0.848	0.394	99
	R ₁₄	All A factors and B factors with FRR	0.711	0.870	0.404	96
	R ₁₅	Selected A factors and B factors with r_{ij}	0.726	0.348	0.667	80
	R ₁₆	Selected A factors and B factors with FR	0.768	0.739	0.442	100
	R ₁₇	Selected A factors B factors with FRR	0.740	0.457	0.600	88

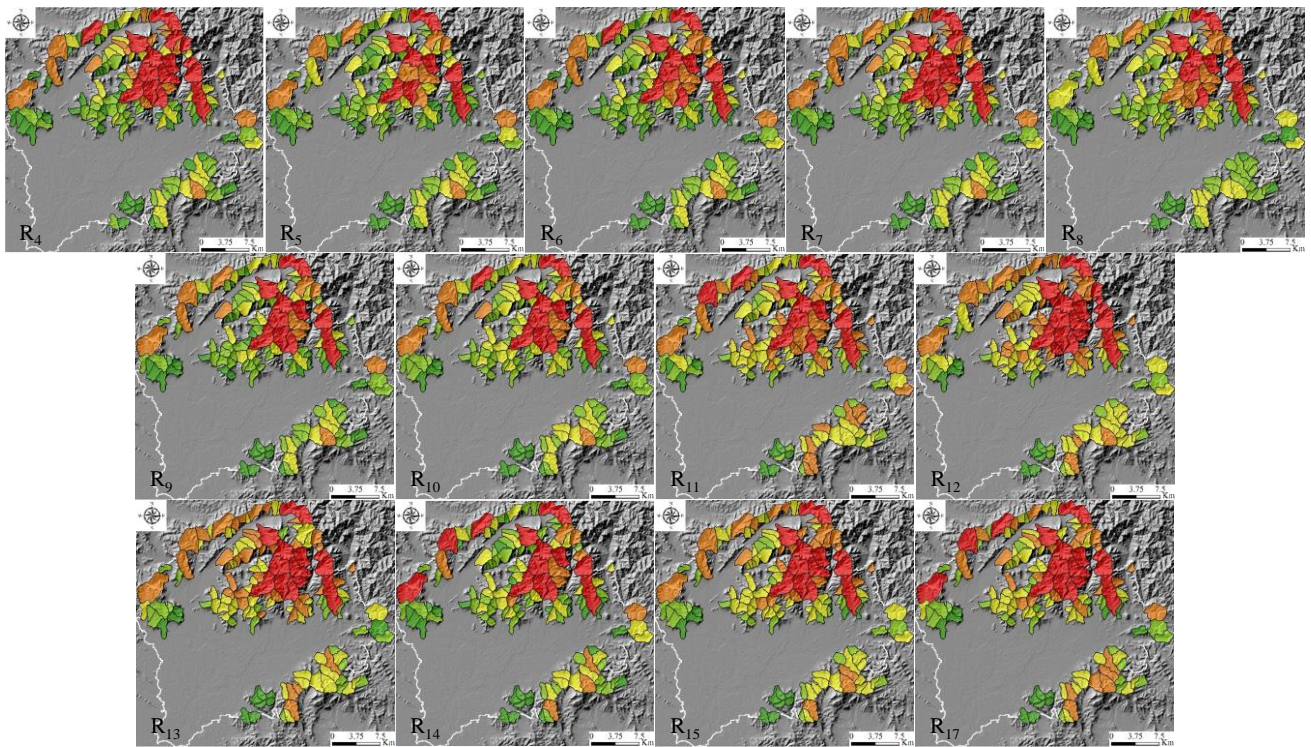
280
281
282

Note: Selected A factors with fuzzy membership more than 0.6; FRR represents the product of FR and r_{ij} ; Performance index is normalized by the largest FR value

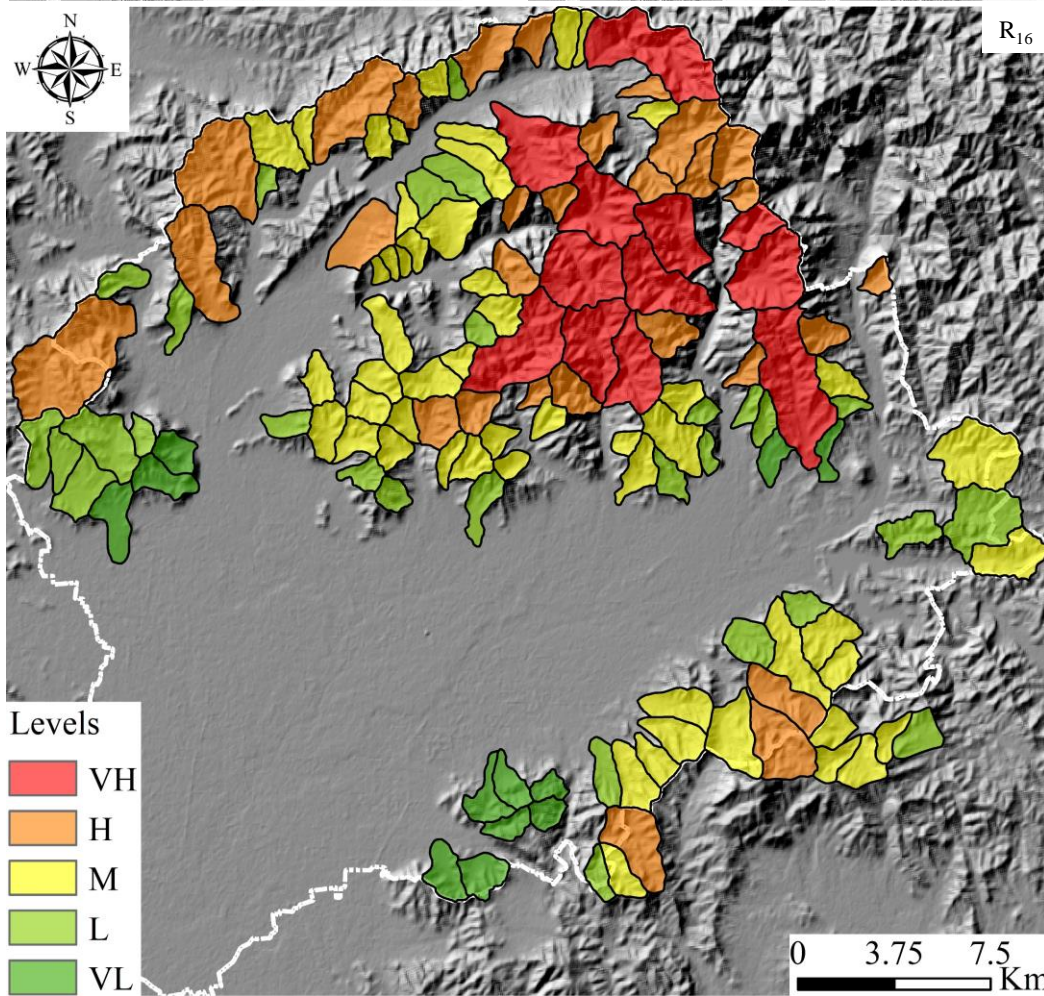


283
284

Fig.7 Results of two categories by Natural Breaks (Jenks) method



285



286

287

Fig. 8 Debris flow susceptibility maps. Note: AUC results of R₁-R₄ below 0.7 were not shown.

288

4 Results and Discussion

289 Through the modelling process, relatively satisfactory results are obtained in this paper. The predictive
290 performance of the output debris flow susceptibility maps, obtained from 17 different models, is verified by
291 comparing with maps published by authority. By comparing the results, the following results are discussed:

292 Firstly, comparing R₁, R₂, R₃, R₄ and R₅, it can be concluded that the model based on field investigation and
293 expert experience is more effective than data-driven directly, when the information is insufficient. This is mainly
294 because when the basin area reaches a certain size, it is no longer controlled by one or several factors, but becomes
295 a complex system. It is not only the factors that affect the system, but also the system will react on each factor.
296 Geomorphic evolution is basically the result of interaction of the endogenic and exogenic geological processes. A
297 geological period can be regarded as the beginning of an endogenic geological processes to the next one. In the early
298 stage of geological period, endogenic geological processes play a major role, and in the later relatively stable period,
299 exogenic geological processes will take on more important parts. In this large cycle, the basin continuously occurs a
300 small cycle of energy accumulating and releasing, which leads to extremely complex system changes. In addition,
301 there is a contradiction between the scale of geological evolution and the scale of engineering activities. So limited
302 information can be obtained under these conditions that leads to the unreliability of data-driven evaluation. Therefore,
303 in the current period, field investigation and expert experience are fundamental.

304 Secondly, by comparing R₄ and R₅, R₆ and R₉, R₇ and R₁₀, R₈ and R₁₁, R₁₂ and R₁₅, R₁₃ and R₁₆, R₁₄ and R₁₇, it
305 can be concluded that the accuracy and resolution of the model can be improved by simplifying the factors, which
306 will eliminate the ones with weak correlation and independence. In practical application, even if the susceptibility
307 map is obtained, the classification of the susceptibility degree is still a very difficult problem. Because everyone's
308 subjective definition of "susceptibility degree" is different. By simplifying the factors, the main ones can be selected,
309 which magnifies the differences between basins, so the boundaries between different susceptibility degrees are more
310 obvious.

311 Thirdly, by comparing R₆ and R₁₂, R₇ and R₁₃, R₈ and R₁₄, R₉ and R₁₅, R₁₀ and R₁₆, R₁₁ and R₁₇, it can be
312 concluded that the model in which factors are classified into two types is better than the one in which all factors as a
313 single thematic layer without classification. Because the factors categorized separately are more closely linked and
314 has consistent influence on the system in mechanism. We can also infer that the non-linear combination characteristics
315 between different types are stronger and scientific classification can improve the performance of the model.

316 Fourthly, comparing R₁₂ and R₁₃, R₁₅ and R₁₆, it can be concluded that the frequency ratio method is better than
317 the cosine amplitude method in the study. Different from the study of (Kritikos and Davies, 2015), the watershed unit
318 rather than the grid unit is used, which indicates that the former has a wide range of application, while the latter has
319 a disadvantage of strict conditions.

320 Based on the results of the above four analyses, the most optimal model should have the features of being based
321 on expert experience, using selected factors, classifying factors before using them, and using frequency ratio method.
322 Then the model R₁₆ is selected according to the features, which is well in accordance with theoretical method
323 performance score, and gets fine mutual verification.

324 There is also much to discuss, the selection of factors is still a very complex dilemma. Although 19 factors
325 selected cannot fully evaluate the character of a basin, it is necessary to consider that they are easily and relatively
326 accurately obtainable for each basin. This will facilitate a wide range of applications. Besides, rainfall and total

327 amount of loose material source are also very important influencing factors. But according to the Beijing hydrological
328 manual, the rainfall change in the study area is not obvious, so it is excluded in model. And the total amount of loose
329 material source cannot be obtained for the watershed without on-site investigation, so calculations are impossible. In
330 fact, we indirectly consider the influence of natural loose material source by evaluating geological conditions, but
331 cannot consider the impact of human activities. As for the factors describing debris flow magnitude, usually, several
332 channels have the recorded data.

333 The scientific and systematic principle of model building is another challenge. To correctly classify the factors,
334 it is necessary to grasp the characteristics of the formation, movement and accumulation of debris flow. Therefore,
335 the classification should comprehensively consider the development background (geology, geomorphology, climate,
336 hydrology, soil, vegetation, human activities and other factors). The practical principle refers to that the study should
337 not only fully obtain scientific and accurate results, but also make the professional results understood by decision
338 makers. Although the susceptibility grade and susceptibility value of each watershed is obtained, the results are
339 relatively effective in this study area. In addition, with the development of technology and theory, we should replace
340 some traditional factors which are not easy to quantify with more precise quantitative factors to improve the efficiency
341 and accuracy of evaluation, such as surface roughness instead of drainage density.

342 For the results derived from Table 3, we would like to further discuss. It can be seen from the results that the
343 occurrence of debris flow is highly correlated with basin volume, basin area and main gully bending coefficient with
344 fuzzy membership above 0.7 in Beijing area. Rainfall in the study area is abundant to induce the debris flow. Loose
345 source and sinks the total volume of catchment become more important. The watershed area determines the total
346 volume of catchment. For the same rainfall, generally, the larger the area, the larger the catchment. The bending
347 coefficient reflects the replenishment sources along the channel. The greater the coefficient, the slower the flow. Then
348 loose source along the channel has more time to replenish. Basin volume characterizes the maximum amount of loose
349 material that can be supplied. These three features reflect the development characteristics of debris flow in the study
350 area. It also provides ideas for disaster prevention and mitigation.

351 Finally, we should consider decision making under uncertainty, because the debris flow phenomenon is
352 extremely complex. The classification of geologists (high, moderate and low) is ambiguous for decision makers. It is
353 more beneficial for them to use mathematically rigorous definitions. Considering that geological conditions tend to
354 vary greatly from region to region, it is not appropriate to define a fixed limit. the Jenks method (chosen in this paper)
355 can be used to classify sensitivity maps according to the characteristics of the data itself. We can also further process
356 the data according to the needs of decision makers, such as identifying 10% of the watersheds in the entire region as
357 high risk. However, the applicability of the model to extreme rainfall and seismic conditions is not considered.

358 **5 Conclusion**

359 In this study, a new combination model for debris-flow susceptibility based on GIS was developed in Pinggu.
360 The objective and motivation of this study is to demonstrate a simple, extensible, and convenient analytical model
361 for the debris flow prediction. Three methods are selected in the model with their own advantages. GRA has great
362 advantages in the case of less samples, data-driven method is mainly used to reduce subjectivity and fuzzy logic is
363 fitted to solve nonlinear problems with fuzzy classification. The output optimal debris flow susceptibility maps

364 demonstrated satisfactory performance with the relative higher susceptibility values corresponding to AUC=0.768.
365 The predictive performance of the susceptibility maps and the spatial correlation of debris flow gully with H and
366 VH susceptibility with recorded debris flows illustrate that the assessment at regional scale using the proposed
367 method is feasible. Compared with the previous results(Li et al., 2020b) based on grid units, the evaluation results
368 are basically the same, but the model are more targeted for debris flow disasters for decision makers. Besides,
369 considering that the meaning of the used factors is clear and the data is easy to obtain, these conditions mentioned
370 enable the model to be widely applied. In addition, a new factor (Basin) is proposed in our study, which contributes
371 higher weight up to 0.79. From our 17 results by comparing the control variables, we suggest that other scholars
372 should pay more attention to the classification and streamlining of factors, which has indicated the potential value
373 to improve model accuracy. It was also found that the watershed characteristic parameters can better reflect the
374 advantages of watershed unit, but further development is needed.

375 In short, an effort has been made to develop a cost- and time-efficient debris flow susceptibility assessment
376 model. The model has an acceptable degree of accuracy for regional-scale planning and contributes to make
377 susceptibility and risk maps more accessible to individuals and local authorities. The GIS-based methods and modern
378 data availability especially through online databases are significantly beneficial to this aim. However, a challenge
379 remains in producing results with practical accuracy for the scale of planning, using available resources. Previous
380 studies highlight that the effectiveness of the final map depends on the quality of input data. Updating and improving
381 existing debris flow catalogues and inventories are crucial for the development of reliable susceptibility and risk
382 assessment methods.

383 **Acknowledgements**

384 This research was financially supported by the Key Project of NSFC-Yunnan Joint Fund (Grant no. U1702241) and
385 the National Key Research and Development Plan (Grant No. 2018YFC1505301). The authors would like to thank Yuchao
386 Li, Zhihai Li, Jiejie Shen, Feifan Gu et al. for their contributions to the collection of field data, and the editor and anonymous
387 reviewers for their comments and suggestions which helped a lot in making this paper better.

388

389 **Reference**

- 390 Akbar, T. A. and Ha, S. R.: Landslide hazard zoning along Himalayan Kaghan Valley of Pakistan—by integration of GPS, GIS, and
391 remote sensing technology, *Landslides*, 8, 527-540, 10.1007/s10346-011-0260-1, 2011.
- 392 Benda, L. E.: Sediment routing by debris flow, 1987.
- 393 Benda, L. E. and Dunne, T.: Sediment routing by debris flow, in: *Erosion and sedimentation in the Pacific Rim*, edited by: Beschta, R.
394 L., Blinn, T., Grant, G. E., Swanson, F. J., and Ice, G. G., IAHS Publ, 213-223, doi:10.1111/j.1753-4887.1977.tb06503.x, 1987.
- 395 The distribution map of potential geological hazard points and susceptibility map in pinggu district:
396 http://ghzrzyw.beijing.gov.cn/zhengwuxinxi/zxzt/dzzhfztt/zzzhdcpj/202008/t20200807_1976436.html, last
397 Borrelli, L., Cofone, G., Coscarelli, R., and Gullà, G.: Shallow landslides triggered by consecutive rainfall events at Catanzaro strait
398 (Calabria–Southern Italy), *Journal of Maps*, 11, 730-744, 10.1080/17445647.2014.943814, 2014.
- 399 Bovis, M. and Dagg, B.: Debris flow triggering by impulsive loading - mechanical modeling and case-studies, *Canadian Geotechnical*
400 *Journal*, 29, 345-352, 10.1139/t92-040, 1992.
- 401 Cao, C., Xu, P., Chen, J., Zheng, L., and Niu, C.: Hazard assessment of debris-flow along the baicha river in heshigten banner, inner
402 mongolia, china, *Int J Environ Res Public Health*, 14, 1-19, 10.3390/ijerph14010030, 2016.
- 403 Chang, T. C. and Chien, Y. H.: The application of genetic algorithm in debris flows prediction, *Environmental Geology*, 53, 339-347,
404 10.1007/s00254-007-0649-2, 2007.
- 405 Chiou, I. J., Chen, C. H., Liu, W. L., Huang, S. M., and Chang, Y. M.: Methodology of disaster risk assessment for debris flows in a
406 river basin, *Stoch Env Res Risk A*, 29, 775-792, 10.1007/s00477-014-0932-1, 2015.
- 407 Chung, C.-J. F. and Fabbri, A. G.: Probabilistic prediction models for landslide hazard mapping, *Photogrammetric Engineering And*
408 *Remote Sensing*, 65, 1389-1399, 10.1016/S0924-2716(99)00030-1, 1999.
- 409 Chung, C. J. F., Fabbri, A., and Westen, C. J. v.: Multivariate regression analysis for landslide hazard zonation, *Geographical*
410 *Information Systems in Assessing Natural Hazards*, 5, 107-133, 1995.
- 411 Conoscenti, C., Ciaccio, M., Caraballo-Arias, N. A., Gómez-Gutiérrez, Á., Rotigliano, E., and Agnesi, V.: Assessment of susceptibility
412 to earth-flow landslide using logistic regression and multivariate adaptive regression splines: A case of the Belice River basin (western
413 Sicily, Italy), *Geomorphology*, 242, 49-64, 10.1016/j.geomorph.2014.09.020, 2015.
- 414 Crozier, M. J., Vaughan, E. E., and Tippett, J. M.: Relative instability of colluvium-filled bedrock depressions, *Earth Surface Processes*
415 *and Landforms*, 15, 329-339, 10.1002/esp.3290150404, 1990.
- 416 Dai, F. C. and Lee, C. F.: Landslide characteristics and slope instability modeling using GIS, Lantau Island, Hong Kong,
417 *Geomorphology*, 42, 213-228, 10.1016/S0169-555X(01)00087-3, 2002.
- 418 Dai, F. C., Lee, C. F., Li, H.-Z., and Xu, C.: Assessment of landslide susceptibility on the natural terrain of Lantau Island, Hong Kong,
419 *Environmental Geology*, 40, 381-391, 10.1007/s002540000163, 2001.
- 420 Deng, J. L.: Control problems of grey systems, *Systems and Control Letters*, 1, 288-294, 10.1016/S0167-6911(82)80025-X, 1982.
- 421 Deng, J. L.: *Grey prediction and decision*, Huazhong University of Science and Technology Press, Wuhan1988.
- 422 Di, B., Zhang, H., Liu, Y., Li, J., Chen, N., Stamatopoulos, C. A., Luo, Y., and Zhan, Y.: Assessing susceptibility of debris flow in
423 southwest china using gradient boosting machine, *Sci Rep*, 9, 12532, 10.1038/s41598-019-48986-5, 2019.
- 424 Di Napoli, M., Carotenuto, F., Cevasco, A., Confuorto, P., Di Martire, D., Firpo, M., Pepe, G., Raso, E., and Calcaterra, D.: Machine
425 learning ensemble modelling as a tool to improve landslide susceptibility mapping reliability, *Landslides*, 17, 1897-1914,
426 10.1007/s10346-020-01392-9, 2020.
- 427 Dietrich, W. E., Wilson, C. J., and Reneau, S. L.: Hollows, colluvium, and landslides in soil-mantled landscapes, in: *Hillslope*
428 *Processes*, edited by: Abrahams., A. D., Allen & Unwin, Boston, 1986.
- 429 Donati, L. and Turrini, M. C.: An objective method to rank the importance of the factors predisposing to landslides with the GIS
430 methodology: application to an area of the Apennines (Valnerina; Perugia, Italy), *Engineering Geology*, 63, 277-289, 10.1016/S0013-
431 7952(01)00087-4, 2002.
- 432 Dong, J.-J., Lee, C.-T., Tung, Y.-H., Liu, C.-N., Lin, K.-P., and Lee, J.-F.: The role of the sediment budget in understanding debris flow

433 susceptibility, *Earth Surface Processes and Landforms*, 34, 1612-1624, 10.1002/esp.1850, 2009.

434 Dramis, F. and Sorriso-Valvo, M.: Deep-seated gravitational slope deformations, related landslides and tectonics, *Engineering Geology*,

435 38, 231-243, 10.1016/0013-7952(94)90040-X, 1994.

436 Ercanoglu, M. and Gokceoglu, C.: Use of fuzzy relations to produce landslide susceptibility map of a landslide prone area (West Black

437 Sea Region, Turkey), *Engineering Geology*, 75, 229-250, 10.1016/j.enggeo.2004.06.001, 2004.

438 Ercanoglu, M. and Temiz, F. A.: Application of logistic regression and fuzzy operators to landslide susceptibility assessment in

439 Azdavay (Kastamonu, Turkey), *Environmental Earth Sciences*, 64, 949-964, 10.1007/s12665-011-0912-4, 2011.

440 Fairchild, L. H.: The importance of lahar initiation processes, *Reviews in Engineering Geology*, 7, 51-62, 10.1130/REG7-p51, 1987.

441 Fang, Z., Wang, Y., Peng, L., and Hong, H.: A comparative study of heterogeneous ensemble-learning techniques for landslide

442 susceptibility mapping, *International Journal of Geographical Information Science*, 35, 321-347, 10.1080/13658816.2020.1808897,

443 2020.

444 Frattini, P., Crosta, G., and Carrara, A.: Techniques for evaluating the performance of landslide susceptibility models, *Engineering*

445 *Geology*, 111, 62-72, 10.1016/j.enggeo.2009.12.004, 2010.

446 Gómez, H. and Kavzoglu, T.: Assessment of shallow landslide susceptibility using artificial neural networks in Jabonosa River Basin,

447 Venezuela, *Engineering Geology*, 78, 11-27, 10.1016/j.enggeo.2004.10.004, 2005.

448 Guzzetti, F., Carrara, A., Cardinali, M., and Reichenbach, P.: Landslide hazard evaluation: a review of current techniques and their

449 application in a multi-scale study, Central Italy, *Geomorphology*, 31, 181-216, 10.1016/s0169-555x(99)00078-1, 1999.

450 He, Y. and Beighley, R. E.: GIS-based regional landslide susceptibility mapping: a case study in southern California, *Earth Surface*

451 *Processes and Landforms*, 33, 380-393, 10.1002/esp.1562, 2008.

452 Hu, K., Wei, F., and Li, Y.: Real-time measurement and preliminary analysis of debris-flow impact force at Jiangjia Ravine, China,

453 *Earth Surface Processes and Landforms*, 36, 1268-1278, 10.1002/esp.2155, 2011.

454 Hungr, O., McDougall, S., and Bovis, M.: Entrainment of material by debris flows, in: *Debris-flow Hazards and Related Phenomena.*,

455 edited by: Jakob, M., and Hungr, O., Praxis.Springer Berlin Heidelberg, 135-158, 2005.

456 Iverson, R. M.: The physics of debris flows, *Reviews of Geophysics*, 35, 245-296., 10.1029/97RG00426, 1997.

457 Iverson, R. M., Reid, M. E., and LaHusen, R. G.: Debris-flow mobilization from landslides, *Annual Review of Earth and Planetary*

458 *Sciences*, 25, 85-138, 10.1146/annurev.earth.25.1.85, 1997.

459 Kanungo, D. P., Arora, M., Sarkar, S., and Gupta, R.: A fuzzy set based approach for integration of thematic maps for landslide

460 susceptibility zonation, *Georisk*, 3, 10.1080/17499510802541417, 2009.

461 Kanungo, D. P., Arora, M. K., Sarkar, S., and Gupta, R. P.: A comparative study of conventional, ANN black box, fuzzy and combined

462 neural and fuzzy weighting procedures for landslide susceptibility zonation in Darjeeling Himalayas, *Engineering Geology*, 85, 347-

463 366, 10.1016/j.enggeo.2006.03.004, 2006.

464 Kellogg, K. S.: Tectonic controls on a large landslide complex: Williams Fork Mountains near Dillon, Colorado, *Geomorphology*, 41,

465 355-368, 10.1016/S0169-555X(01)00067-8, 2001.

466 Khan, U., Tuteja, N. K., and Sharma, A.: Delineating hydrologic response units in large upland catchments and its evaluation using soil

467 moisture simulations, *Environmental Modelling & Software*, 46, 142-154, 10.1016/j.envsoft.2013.03.005, 2013.

468 Khan, U., Tuteja, N. K., Sharma, A., Lucas, S., Murphy, B., and Jenkins, B.: Applicability of Hydrologic Response Units in low

469 topographic relief catchments and evaluation using high resolution aerial photograph analysis, *Environmental Modelling & Software*,

470 81, 56-71, 10.1016/j.envsoft.2016.03.010, 2016.

471 Korup, O.: Geomorphic implications of fault zone weakening Slope instability along the Alpine Fault South Westland to Fiordland,

472 *New Zealand Journal of Geology and Geophysics*, 47, 257-267, 10.1080/00288306.2004.9515052, 2004.

473 Kritikos, T. and Davies, T.: Assessment of rainfall-generated shallow landslide/debris-flow susceptibility and runoff using a GIS-based

474 approach: application to western Southern Alps of New Zealand, *Landslides*, 12, 1051-1075, 10.1007/s10346-014-0533-6, 2015.

475 Kuo, Y., Yang, T., and Huang, G.-W.: The use of grey relational analysis in solving multiple attribute decision-making problems,

476 *Computers & Industrial Engineering*, 55, 80-93, 10.1016/j.cie.2007.12.002, 2008.

477 Lee, S.: Application and verification of fuzzy algebraic operators to landslide susceptibility mapping, *Environmental Geology*, 52, 615-
478 623, 10.1007/s00254-006-0491-y, 2006.

479 Lee, S. and Choi, J.: Landslide susceptibility mapping using GIS and the weight-of-evidence model, *International Journal of*
480 *Geographical Information Science*, 18, 789-814, 10.1080/13658810410001702003, 2004.

481 Lee, S. and Sambath, T.: Landslide susceptibility mapping in the Damrei Romel area, Cambodia using frequency ratio and logistic
482 regression models, *Environmental Geology*, 50, 847-855, 10.1007/s00254-006-0256-7, 2006.

483 Lee, S. and Talib, J. A.: Probabilistic landslide susceptibility and factor effect analysis, *Environmental Geology*, 47, 982-990,
484 10.1007/s00254-005-1228-z, 2005.

485 Lee, S., Ryu, J.-H., Min, K., and Won, J.-S.: Landslide susceptibility analysis using GIS and artificial neural network, *Earth Surface*
486 *Processes and Landforms*, 28, 1361-1376, 10.1002/esp.593, 2003.

487 Li, Y., Chen, J., Zhang, Y., Song, S., Han, X., and Ammar, M.: Debris flow susceptibility assessment and runout prediction: A case
488 study in shiyang gully, beijing, china, *International Journal of Environmental Research*, 14, 365-383, 10.1007/s41742-020-00263-4,
489 2020a.

490 Li, Y., Chen, J., Li, Z., Han, X., Zhai, S., Li, Y., and Zhang, Y.: A case study of debris flow risk assessment and hazard range prediction
491 based on a neural network algorithm and finite volume shallow water flow model, *Environmental Earth Sciences*, 80, 10.1007/s12665-
492 021-09580-z, 2021a.

493 Li, Y., Chen, J., Tan, C., Li, Y., Gu, F., Zhang, Y., and Mehmood, Q.: Application of the borderline-SMOTE method in susceptibility
494 assessments of debris flows in Pinggu District, Beijing, China, *Natural Hazards*, 105, 2499-2522, 10.1007/s11069-020-04409-7,
495 2020b.

496 Li, Z., Chen, J., Tan, C., Zhou, X., Li, Y., and Han, M.: Debris flow susceptibility assessment based on topo-hydrological factors at
497 different unit scales: a case study of Mentougou district, Beijing, *Environmental Earth Sciences*, 80, 10.1007/s12665-021-09665-9,
498 2021b.

499 Liang, W.-j., Zhuang, D.-f., Jiang, D., Pan, J.-j., and Ren, H.-y.: Assessment of debris flow hazards using a Bayesian Network,
500 *Geomorphology*, 171-172, 94-100, 10.1016/j.geomorph.2012.05.008, 2012.

501 Lin, C. L. and Lin, C. L.: The use of the orthogonal array with grey relational analysis to optimize the electrical discharge machining
502 process with multiple performance characteristics, *International Journal of Machine Tools and Manufacture*, 42, 237-244,
503 10.1016/S0890-6955(01)00107-9, 2002.

504 Liu, L. and Wang, S.: Fuzzy comprehensive evaluation on landslide and debris flow risk degree in Zaotong, Yunnan, *Mountain*
505 *Research*, 13, 261-266, 1995.

506 Liu, S., Dang, Y., and Fang, Z.: *Grey system theory and its applications*, Science Press, Beijing 2004.

507 Liu, Y., Guo, H. C., Zou, R., and Wang, L. J.: Neural network modeling for regional hazard assessment of debris flow in Lake
508 Qionghai Watershed, China, *Environmental Geology*, 49, 968-976, 10.1007/s00254-005-0135-7, 2005.

509 Lü, J., Wang, C., Liu, H., and Zhang, X.: Division of beijing geological environment system, *Urban geology*, 12, 19-25,
510 10.3969/j.issn.1007-1903.2017.03.004, 2017.

511 Luo, X. and Dimitrakopoulos, R.: Data-driven fuzzy analysis in quantitative mineral resource assessment, *Computers & Geosciences*,
512 29, 3-13, 10.1016/s0098-3004(02)00078-x, 2003.

513 Marjanović, M., Kovačević, M., Bajat, B., and Voženílek, V.: Landslide susceptibility assessment using SVM machine learning
514 algorithm, *Engineering Geology*, 123, 225-234, 10.1016/j.enggeo.2011.09.006, 2011.

515 Melo, R., Vieira, G., Caselli, A., and Ramos, M.: Susceptibility modelling of hummocky terrain distribution using the information
516 value method (Deception Island, Antarctic Peninsula), *Geomorphology*, 155-156, 88-95, 10.1016/j.geomorph.2011.12.027, 2012.

517 Meyer, N. K., Schwanghart, W., Korup, O., Romstad, B., and Etzelmüller, B.: Estimating the topographic predictability of debris
518 flows, *Geomorphology*, 207, 114-125, 10.1016/j.geomorph.2013.10.030, 2014.

519 Ohlmacher, G. C.: Plan curvature and landslide probability in regions dominated by earth flows and earth slides, *Engineering Geology*,
520 91, 117-134, 10.1016/j.enggeo.2007.01.005, 2007.

521 Pierson, T. C., Janda, R. J., Thouret, J.-C., and Borrero, C. A.: Perturbation and melting of snow and ice by the 13 November 1985
522 eruption of Nevado del Ruiz, Colombia, and consequent mobilization, flow and deposition of lahars, *Journal of Volcanology and*
523 *Geothermal Research*, 41, 17-66, 10.1016/0377-0273(90)90082-q, 1990.

524 Porwal, A., Carranza, E. J. M., and Hale, M.: A Hybrid Fuzzy Weights-of-Evidence Model for Mineral Potential Mapping, *Natural*
525 *Resources Research*, 15, 1-14, 10.1007/s11053-006-9012-7, 2006.

526 Pourghasemi, H. R., Yousefi, S., Kornejady, A., and Cerda, A.: Performance assessment of individual and ensemble data-mining
527 techniques for gully erosion modeling, *Sci Total Environ*, 609, 764-775, 10.1016/j.scitotenv.2017.07.198, 2017.

528 Pradhan, B.: Landslide susceptibility mapping of a catchment area using frequency ratio, fuzzy logic and multivariate logistic
529 regression approaches, *Journal of the Indian Society of Remote Sensing*, 38, 301-320, 10.1007/s12524-010-0020-z, 2010.

530 Pradhan, B.: Manifestation of an advanced fuzzy logic model coupled with Geo-information techniques to landslide susceptibility
531 mapping and their comparison with logistic regression modelling, *Environmental and Ecological Statistics*, 18, 471-493,
532 10.1007/s10651-010-0147-7, 2011a.

533 Pradhan, B.: Use of GIS-based fuzzy logic relations and its cross application to produce landslide susceptibility maps in three test
534 areas in Malaysia, *Environmental Earth Sciences*, 63, 329-349, 10.1007/s12665-010-0705-1, 2011b.

535 Regmi, N. R., Giardino, J. R., McDonald, E. V., and Vitek, J. D.: A comparison of logistic regression-based models of susceptibility to
536 landslides in western Colorado, USA, *Landslides*, 11, 247-262, 10.1007/s10346-012-0380-2, 2013.

537 Remondo, J., González, A., Terán, J. R. D. D., Cendrero, A., Fabbri, A., and Chung, C.-J. F.: Validation of landslide susceptibility
538 maps; examples and applications from a case study in northern Spain, *Natural Hazards*, 30, 437-449,
539 10.1023/B:NHAZ.0000007201.80743.fc, 2003.

540 Roeloffs, E.: Poroelastic techniques in the study of earthquake-related hydrologic phenomena, 38, 135-195, 10.1016/S0065-
541 2687(08)60270-8, 1996.

542 Ross, T. J.: *Fuzzy logic with engineering applications*, McGraw-Hill, New York 1995.

543 Selby, M. J.: *Hillslope materials and processes*, Oxford University Press, Oxford 1982.

544 Sun, X., Chen, J., Bao, Y., Han, X., Zhan, J., and Peng, W.: Landslide Susceptibility Mapping Using Logistic Regression Analysis
545 along the Jinsha River and Its Tributaries Close to Derong and Deqin County, Southwestern China, *ISPRS International Journal of*
546 *Geo-Information*, 7, 10.3390/ijgi7110438, 2018.

547 Takahashi, T.: *Debris flow mechanics, prediction and countermeasures*, second, Taylor & Francis/Balkema, The Netherlands 2014.

548 Tien Bui, D., Pradhan, B., Lofman, O., Revhaug, I., and Dick, O. B.: Landslide susceptibility assessment in the Hoa Binh province of
549 Vietnam: A comparison of the Levenberg–Marquardt and Bayesian regularized neural networks, *Geomorphology*, 171-172, 12-29,
550 10.1016/j.geomorph.2012.04.023, 2012.

551 Tsangaratos, P. and Ilia, I.: Landslide susceptibility mapping using a modified decision tree classifier in the Xanthi Prefecture, Greece,
552 *Landslides*, 13, 305-320, 10.1007/s10346-015-0565-6, 2015.

553 Tsukamoto, Y., Ohta, T., and Noguchi, H.: Hydrological and geomorphological studies of debris slides on forested hillslopes in Japan,
554 *Journal des Sciences Hydrologiques*, 27, 234, 1982.

555 Vallance, J. W. and Scott, K. M.: The Osceola mudflow from Mount Rainier: Sedimentology and hazard implications of a huge clay-
556 rich debris flow, *Geological Society of America Bulletin*, 109, 143-163, 10.1130/0016-7606(1997)109<0143:TOMFMR>2.3.CO;2,
557 1997.

558 Wang, J., Yu, Y., Yang, S., Lu, G.-h., and Ou, G.-q.: A modified certainty coefficient method (M-CF) for debris flow susceptibility
559 assessment: A case study for the Wenchuan earthquake meizoseismic areas, *Journal of Mountain Science*, 11, 1286-1297,
560 10.1007/s11629-013-2781-7, 2014.

561 Wei, Z., Shang, Y., Zhao, Y., Pan, P., and Jiang, Y.: Rainfall threshold for initiation of channelized debris flows in a small catchment
562 based on in-site measurement, *Engineering Geology*, 217, 23-34, 10.1016/j.enggeo.2016.12.003, 2017.

563 Westen, C. J. v., Rengers, N., and Soeters, R.: Use of geomorphological information in indirect landslide susceptibility assessment,
564 *Natural Hazards*, 30, 399-419, 10.1023/B:NHAZ.0000007097.42735.9e, 2003.

565 Wu, S., Chen, J., Zhou, W., Iqbal, J., and Yao, L.: A modified Logit model for assessment and validation of debris-flow susceptibility,
566 Bulletin of Engineering Geology and the Environment, 78, 4421-4438, 10.1007/s10064-018-1412-5, 2019.

567 Wu, Y., Li, W., Liu, P., Bai, H., Wang, Q., He, J., Liu, Y., and Sun, S.: Application of analytic hierarchy process model for landslide
568 susceptibility mapping in the Gangu County, Gansu Province, China, Environmental Earth Sciences, 75, 10.1007/s12665-015-5194-9,
569 2016.

570 Xie, H., Zhong, D., Wei, F., and Wang, S.: Classification of debris flow in the mountains of Beijing, Journal of mountain science, 22,
571 212-219, 10.16089/j.cnki.1008-2786.2004.02.013, 2004.

572 Zadeh, L. A.: Fuzzy sets, Information & Control, 8, 338-353, 10.1016/S0019-9958(65)90241-X, 1965.

573 Zhang, W., Li, H. Z., Chen, J. p., Zhang, C., Xu, L. m., and Sang, W. f.: Comprehensive hazard assessment and protection of debris
574 flows along Jinsha River close to the Wudongde dam site in China, Natural Hazards, 58, 459-477, 10.1007/s11069-010-9680-9, 2011.

575 Zhang, W., Chen, J.-p., Wang, Q., An, Y., Qian, X., Xiang, L., and He, L.: Susceptibility analysis of large-scale debris flows based on
576 combination weighting and extension methods, Natural Hazards, 66, 1073-1100, 10.1007/s11069-012-0539-0, 2013.

577 Zhang, Y., Chen, J., Tan, C., Bao, Y., Han, X., Yan, J., and Mehmood, Q.: A novel approach to simulating debris flow runout via a
578 three-dimensional CFD code: a case study of Xiaojia Gully, Bulletin of Engineering Geology and the Environment, 80, 5293-5313,
579 10.1007/s10064-021-02270-x, 2021.

580 Zhong, D., Xie, H., Wang, S., Wei, F., and Jin, H.: Debris flow in Beijing mountain, Commercial Press, Beijing 2004.

581 Zou, Q., Cui, P., He, J., Lei, Y., and Li, S.: Regional risk assessment of debris flows in China—An HRU-based approach,
582 Geomorphology, 340, 84-102, 10.1016/j.geomorph.2019.04.027, 2019.

583